$SrCo_2Sn_8$ and $BaCo_2Sn_8$: Tin-rich Stannides with Distorted $SnSn_6$ Octahedra within Three-dimensional $[Co_2Sn_8]$ Networks

Christian Schwickert and Rainer Pöttgen

Institut für Anorganische und Analytische Chemie, Universität Münster, Corrensstrasse 30, 48149 Münster, Germany

Reprint requests to R. Pöttgen. E-mail: pottgen@uni-muenster.de

Z. Naturforsch. **2013**, *68b*, 17 – 22 / 10.5560/ZNB.2013-2293
Received November 7, 2012

The tin-rich stannides $SrCo_2Sn_8$ and $BaCo_2Sn_8$ were synthesized from the elements in sealed tantalum tubes. They crystallize with a new structure type, space group *Cccm* with $a = 1006.0(3)$, $b = 1514.4(6)$, $c = 1385.0(6)$ pm for $SrCo_2Sn_8$ and $a = 1032.8(2)$, $b = 1516.8(3)$, $c = 1405.1(3)$ pm for $BaCo_2Sn_8$. The structure of the barium compound was refined on the basis of single-crystal X-ray diffractometer data: $wR2 = 0.0450$, 1715 F^2 values, 57 variables. The cobalt atoms have seven nearest tin neighbors with Co–Sn distances ranging from 257 to 273 pm. These $CoSn_7$ units are condensed *via* common rectangular faces to $[Co_2Sn_{10}]$ double units which build up a covalently bonded three-dimensional network through Sn–Co–Sn bridges. Larger voids left by this network are filled by the barium and the Sn2 atoms. The latter have distorted octahedral tin coordination with Sn2–Sn distances of 311 – 315 pm. The barium atoms have 13 nearest tin neighbors (352 – 399 pm Ba–Sn). Temperature-dependent magnetic susceptibility data of $BaCo_2Sn_8$ show Pauli paramagnetism.

Key words: Stannide, Crystal Structure, Pauli Paramagnetism, Cobalt, Strontium, Barium

Introduction

Cobalt and tin form the binary stannides Co_3Sn_2 [1], CoSn, $CoSn_2$ [2], and two modifications of $CoSn_3$ [3]. The stability of these stannides results from covalent Co–Sn and also from Sn–Sn bonding (in the tin-rich phases). The structural diversity of cobalt stannides is significantly increased if a third, more electropositive metal is present. So far more than 90 $RE_xCo_ySn_z$ stannides (RE = rare earth element) with different crystal structures and a broad variety of magnetic and electrical properties have been reported. An overview is given in a review article by Skolozdra [4]. Especially the tin-rich phases have intensively been studied since they are readily available in single-crystalline form through self-flux synthesis [5].

Despite the large number of $RE_xCo_ySn_z$ stannides, only few analogs with alkali or alkaline earth metals have been reported [6, 7]. The only known ternary lithium compound is $LiCoSn_6$ [8, 9]. The cobalt atoms in $LiCoSn_6$ have similar square-antiprismatic coordination as in $CoSn_2$ and $CoSn_3$. The second alkali metal stannide is the recently reported Zintl phase $K_{5-x}Co_{1-x}Sn_9$ with endohedral $[Co@Sn_9]^{5-}$ cluster units [10]. The structure of $Mg_2Co_3Sn_{10+x}$ [11] has cobalt in two different coordinations. The Co1 atoms have coordination number (CN) 8 in a square-antiprismatic fashion, and Co2 has CN 6 in the form of trigonal prisms. A high-pressure study in a diamond anvil cell showed stability of the $Mg_2Co_3Sn_{10+x}$ structure up to 9 GPa [12].

Ternary stannides $RE_3T_4Sn_{13}$ have intensively been studied in the 1980s with respect to their superconducting and magnetic properties [13, 14]. These cubic phases were also observed for $Ca_3Co_4Sn_{13}$ and $Sr_3Co_4Sn_{13}$. The calcium compound shows a superconducting transition at 5.9 K. The structure is composed of a three-dimensional network of $CoSn_6$ trigonal prisms which are condensed *via* common corners. The cavities left by this network are filled by calcium and additional tin atoms. Recent single-crystal investigation [15] revealed a composition $Ca_{3+x}Co_4Sn_{13-x}$, resulting from Ca/Sn mixing on the 2*a* site, frequently observed for this structure type [16].

Herein we report on the first ternary cobalt stannides with strontium and barium, $SrCo_2Sn_8$ and $BaCo_2Sn_8$,

which are among the tin-richest ternary phases with a pronounced tin substructure.

Experimental

Synthesis

Lath-shaped single crystals of $BaCo_2Sn_8$ were first obtained as a by-product when searching for ternary barium-cobalt-phosphides using the tin flux technique [5]. Starting materials for the targeted synthesis of $SrCo_2Sn_8$ and $BaCo_2Sn_8$ were strontium (Sigma Aldrich, 99 %) and barium rods (Alfa Aesar, > 99 %), cobalt powder (Sigma Aldrich, 99.9 %), and tin granules (Merck, 99.9 %). Polycrystalline samples were prepared by weighing the elements in the ideal ratios and placing them in tantalum ampoules [17] under an argon atmosphere of *ca.* 700 mbar. The argon was purified over titanium sponge (900 K), silica gel, and molecular sieves. Suitable barium and strontium pieces were prepared under paraffin oil and kept in a Schlenk tube under argon atmosphere. The tantalum ampoules were then sealed in evacuated silica tubes and placed in a resistance furnace. They were heated to 1100 K within 12 h and kept at that temperature for 48 h. The tubes were then slowly cooled to 650 K, kept at that temperature for another 168 h and afterwards cooled to ambient temperature by radiative heat loss. The resulting ingots are ductile and exhibit silver luster whereas ground powders are light grey. The samples are stable for months.

First synthesis attempts were performed in niobium ampoules, but the high tin content led to an attack of the crucible material. Well-shaped single crystals of recrystallized niobium, equiatomic NbCoSn and an unknown barium-niobium-stannide were observed as by-products. Further investigations on the new ternary barium stannide are in progress.

EDX data

Semiquantitative EDX analyses of the single crystal studied on the diffractometer were carried out in variable pressure mode with a Zeiss EVO® MA10 scanning electron microscope with BaF_2, Co and Sn as standards. The experimentally observed average composition of 9 ± 1 at.-% Ba : 17 ± 1 at.-% Co : 74 ± 1 at.-% Sn for the lath-shaped single crystals (Fig. 1) were close to the ideal one (9.1 : 17.2 : 72.7). No impurity elements, especially from the container material, were detected.

X-Ray diffraction

The polycrystalline $SrCo_2Sn_8$ and $BaCo_2Sn_8$ samples were characterized by Guinier patterns (imaging plate detector, Fujifilm BAS-1800) with Cu$K_{\alpha 1}$ radiation and α-quartz

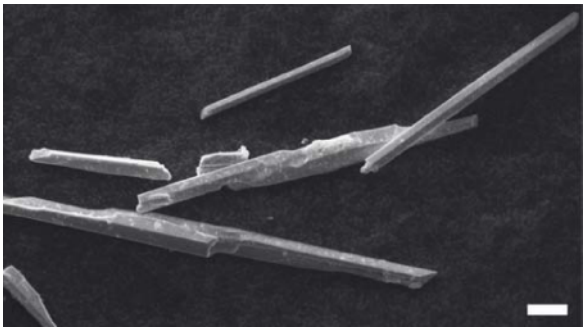

Fig. 1. Scanning electron micrograph of lath-shaped $BaCo_2Sn_8$ crystals. The white bar at the lower right-hand side corresponds to a length of 20 μm.

Table 1. Lattice parameters for the stannides $AECo_2Sn_8$.

Compound	a (pm)	b (pm)	c (pm)	V (nm^3)
$SrCo_2Sn_8$	1006.0(3)	1514.4(6)	1385.0(6)	2.1100
$BaCo_2Sn_8$	1032.8(2)	1516.8(3)	1405.1(3)	2.2012

($a = 491.30$, $c = 540.46$ pm) as an internal standard. The orthorhombic lattice parameters (Table 1) were obtained from a least-squares refinement. Proper indexing was ensured through intensity calculations [18]. The single-crystal and powder lattice parameters of the barium compound agreed well.

Lath-shaped singe crystals of $BaCo_2Sn_8$ were selected from the carefully crushed sample, glued to quartz fibers using beeswax and studied on a Buerger camera (using white Mo radiation) to check their quality. The intensity data collection was performed on a Stoe IPDS-II image plate system (graphite monochromatized MoK_α radiation; $\lambda = 71.073$ pm) in oscillation mode. A numerical absorption correction was applied to the data. Details about the data collection and the crystallographic parameters are summarized in Table 2.

Structure determination and refinement

The $BaCo_2Sn_8$ data set showed a *C*-centered orthorhombic lattice, and the systematic extinction conditions were in agreement with the centrosymmetric space group *Cccm*. The starting atomic parameters were deduced from Direct Methods with SHELXS-97 [19, 20], and the structure was refined with anisotropic displacement parameters for all atoms with SHELXL-97 (full-matrix least-squares on F_o^2) [21, 22]. To check for deviations from the ideal composition, the occupancy parameters were refined in a separate series of least-squares cycles. All sites were fully occupied within two standard deviations. The final difference Fourier syntheses revealed no residual peaks. The refined atomic positions,

Table 2. Crystal data and structure refinement for $BaCo_2Sn_8$.

Empirical formula	$BaCo_2Sn_8$
Formula weight, g mol^{-1}	1204.72
Unit cell dimension	Table 1
Space group, Z	*Cccm*, 8
Calculated density, g cm^{-3}	7.27
Crystal size, μm^3	$10 \times 10 \times 180$
Transmission ratio (min / max)	0.255 / 0.833
Absorption coefficient, mm^{-1}	24.2
$F(000)$, e	4080
θ range for data collection, deg	2–31
Range in *hkl*	±14, ±21, ±19
Total no. of reflections	22 617
Independent reflections / R_{int}	1715 / 0.1457
Reflections with $I > 2\sigma(I)/R_\sigma$	1029 / 0.0997
Data / parameters	1715 / 57
Goodness-of-fit on F^2	0.849
$R1$ / $wR2$ for $I > 2\sigma(I)$	0.0428 / 0.0363
$R1$ / $wR2$ for all data	0.1115 / 0.0450
Extinction coefficient	0.000043(3)
Largest diff. peak / hole, e Å^{-3}	2.90 / −2.03

Table 3. Atomic coordinates and equivalent isotropic displacement parameters (pm^2) for $BaCo_2Sn_8$. U_{eq} is defined as one third of the trace of the orthogonalized U_{ij} tensor.

Atom	Site	x	y	z	U_{eq}
Ba	8*l*	0.05156(10)	0.15409(9)	0	149(2)
Co	16*m*	0.57418(12)	0.14641(11)	0.17002(10)	84(3)
Sn1	8*l*	0.50786(13)	0.09669(8)	0	113(2)
Sn2	4*a*	0	0	1/4	179(4)
Sn3	8*h*	1/2	0.29517(7)	1/4	131(3)
Sn4	8*k*	3/4	1/4	0.10515(10)	103(3)
Sn5	16*m*	0.30991(7)	0.15256(6)	0.16355(5)	123(2)
Sn6	16*m*	0.76485(9)	0.04106(5)	0.11455(7)	144(2)
Sn7	4*b*	1/2	0	1/4	97(3)

equivalent isotropic and anisotropic displacement parameters, and interatomic distances are given in Tables 3–4.

Further details of the crystal structure investigation may be obtained from Fachinformationszentrum Karlsruhe, 76344 Eggenstein-Leopoldshafen, Germany (fax: +49-7247-808-666; E-mail: crysdata@fiz-karlsruhe.de, http://www.fiz-karlsruhe.de/request_for_deposited_data.html) on quoting the deposition number CSD-425335.

Magnetic susceptibility measurements

Magnetic measurements were carried out on a Quantum Design Physical Property Measurement System using the VSM option. 70.773 mg of the $BaCo_2Sn_8$ sample were packed in a polypropylene capsule and attached to the sample holder rod. The measurement was performed in the temperature range of 3 – 350 K with magnetic flux densities up to 10 kOe.

Table 4. Anisotropic displacement parameters (pm^2) for $BaCo_2Sn_8$.

Atom	U_{11}	U_{22}	U_{33}	U_{12}	U_{13}	U_{23}
Ba	102(4)	225(5)	121(4)	−15(5)	0	0
Co	89(7)	81(6)	82(6)	−23(7)	3(6)	8(7)
Sn1	135(5)	127(5)	76(5)	−20(5)	0	0
Sn2	136(8)	185(8)	218(9)	0	0	0
Sn3	180(7)	80(5)	132(6)	0	13(6)	0
Sn4	94(6)	110(6)	106(6)	−47(5)	0	0
Sn5	100(4)	144(3)	126(3)	13(4)	−42(3)	−6(4)
Sn6	118(4)	135(4)	178(4)	33(3)	16(4)	1(4)
Sn7	117(8)	66(7)	109(8)	0	0	0

Discussion

Crystal chemistry

The tin-rich stannides $SrCo_2Sn_8$ and $BaCo_2Sn_8$ crystallize in a new structure type (space group *Cccm*, Pearson code oC88) with a metal-to-tin ratio of 1 : 2.66. Among the huge number of ternary alkaline earth- and rare earth-transition metal stannides they are among those with the highest tin content. The lattice parameters of the strontium compound are smaller than those of $BaCo_2Sn_8$. Although this structure type is governed by a complex three-dimensional $[Co_2Sn_8]$ network, even the small change in the size of the alkaline earth metal leads to an anisotropic expansion of the unit cell, much more pronounced in the *a* and *c* as compared to the *b* axis.

The shortest interatomic distances in the $BaCo_2Sn_8$ structure occur between the cobalt and tin atoms. Each cobalt atom has seven nearest tin neighbors with Co–Sn distances ranging from 257 to 273 pm, close to the sum of the covalent radii [23] of 256 pm. This is indicative of strong covalent Co–Sn bonding. The near-neighbor coordination of the cobalt atoms is presented in Fig. 2. The Co–Sn distances observed in $BaCo_2Sn_8$ compare well with those in $Dy_3Co_6Sn_5$ (257 – 274 pm) [24], $Mg_2Co_3Sn_{10+x}$ (260 – 277 pm) [11], $La_4Co_2Sn_5$ (259 – 273 pm) [25], or Yb_3CoSn_6 (250 – 255 pm) [26].

The $Co@Sn_7$ units are condensed *via* a common rectangular face formed by the Sn3, Sn5 (2×) and Sn7 atoms. Within the double units one observes a Co–Co distance of 272 pm, longer than in *hcp* Co (6×250 and 6×251 pm) [27]. The $Co_2@Sn_{10}$ double units resemble the $Co_2@Sn_{12}$ units (two condensed square antiprisms) of $CoSn_2$ [2] and $CoSn_3$ [3]. The Co–Co distances are 272 pm in $CoSn_2$ and 269 and 270 pm in

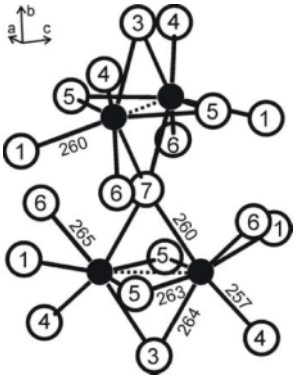

Fig. 2. The near neighbor coordination of the cobalt atoms in the structure of $BaCo_2Sn_8$. Cobalt and tin atoms are drawn as black filled, and open circles, respectively. Atom designations and relevant interatomic distances are indicated.

the two modifications of $CoSn_3$. These Co–Sn interactions are considered as only weakly bonding. Two $Co_2@Sn_{10}$ double units are connected *via* the common Sn7 atoms to tetrameric units, and the latter further condense *via* the Sn4 atoms, leading to the three-dimensional network presented in Fig. 3.

As expected for a tin-rich stannide, one observes a broad range of Sn–Sn distances (294 – 386 pm) in the structure of $BaCo_2Sn_8$. The shortest Sn–Sn distance of 294 pm occurs between the Sn1 atoms. This short Sn1–Sn1 distance certainly corresponds to a strong bond. It is close to the Sn–Sn distance of 281 in the diamond modification of α-Sn [27]. Most of the longer Sn–Sn distances fit well with those in the β-Sn structure (4×302 and 2×318 pm) [27] and furthermore, one observes a variety of secondary, weak Sn–Sn interactions. This is expected for the complex crystal structure with seven crystallographically independent tin sites. Comparable Sn–Sn distances occur in further tin-rich stannides, *e. g.* $Ce_3Rh_4Sn_{13}$ (299 – 334 pm) [28] or $CaRhSn_2$ (303 – 322 pm) [29].

A remarkable structural feature concerns the tin substructure. The Sn2 atoms (Wyckoff site 4*a*) have no cobalt neighbors and are not part of the three-dimensional $[Co_4Sn_{15} \equiv Co_2Sn_{7.5}]$ network. They have six tin neighbors (311 – 315 pm) in distorted octahedral coordination (Fig. 4). These $SnSn_6$ octahedra are a new structural motif in polystannide chemistry, and there is no counterpart in molecular chemistry. Parts of the octahedra resemble the square-pyramidal Sn_5^{6-} Zintl anion in Ba_3Sn_5 (299 – 315 pm Sn–Sn) [30]. Other tin motifs in ternary polystannides are zig-zag chains (Yb_3CoSn_6 [26]), lonsdaleite-related tetrahedral networks ($CaRhSn_2$ [29]), icosahedra ($Ce_3Rh_4Sn_{13}$ [28]), or cyclohexane-type rings ($Mg_2Co_3Sn_{10+x}$ [11]).

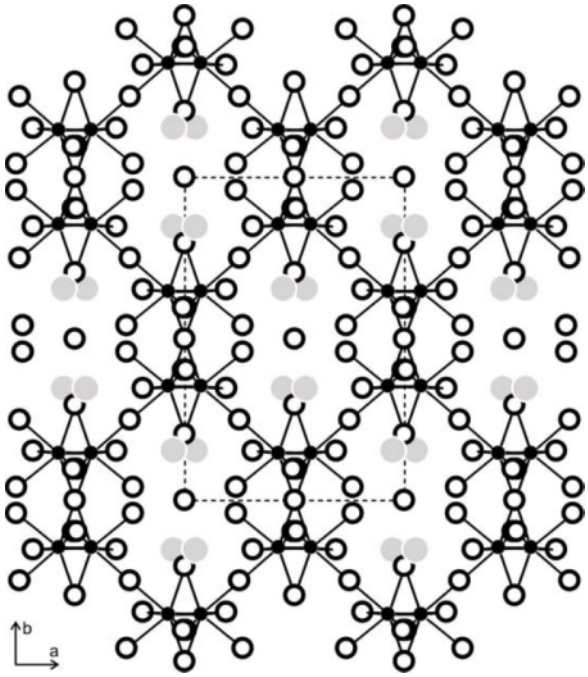

Fig. 3. Projection of the $BaCo_2Sn_8$ structure along the *c* axis. Barium, cobalt and tin atoms are drawn as medium grey, black filled, and open circles, respectively. The Co_2 dumbbells and the Co–Sn bonds are emphasized.

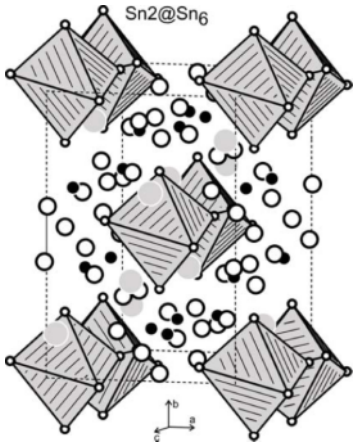

Fig. 4. View of the $BaCo_2Sn_8$ structure approximately along the *c* axis. Barium, cobalt and tin atoms are drawn as medium grey, black filled, and open circles, respectively. The distorted $Sn2@Sn_6$ octahedra are emphasized.

Table 5. Interatomic distances (pm), for $BaCo_2Sn_8$ calculated with the powder lattice parameters. Standard deviations are equal to or smaller than 0.2 pm. All distances of the first coordination spheres are listed.

Ba:	2	Sn5	352.2	Sn4:	2	Co	256.8
	2	Sn3	363.5		1	Sn4	295.5
	2	Sn4	374.2		2	Sn6	317.6
	2	Sn6	378.1		2	Sn3	335.8
	1	Sn1	383.0		2	Sn5	362.4
	2	Sn6	386.6		2	Sn1	372.1
	2	Sn5	399.1		2	Ba	374.2
Co:	1	Sn4	256.9	Sn5:	1	Co	262.9
	1	Sn1	259.7		1	Co	273.3
	1	Sn7	260.4		1	Sn6	311.4
	1	Sn5	262.9		1	Sn3	316.4
	1	Sn3	263.5		1	Sn1	319.0
	1	Sn6	265.3		1	Sn5	320.5
	1	Co	272.0		1	Sn7	326.9
	1	Sn5	273.3		1	Sn3	351.4
Sn1:	2	Co	259.7		1	Ba	352.1
	1	Sn1	293.8		1	Sn4	362.4
	2	Sn5	319.0		1	Sn6	363.0
	2	Sn6	321.7		1	Ba	399.1
	2	Sn4	372.1	Sn6:	1	Co	265.3
	2	Sn7	380.8		1	Sn5	311.4
	1	Ba	383.0		1	Sn2	314.8
Sn2:	2	Sn3	310.7		1	Sn4	317.6
	4	Sn6	314.8		1	Sn1	321.7
Sn3:	2	Co	263.5		1	Sn6	321.9
	1	Sn2	310.7		1	Sn7	339.0
	2	Sn5	316.4		1	Sn5	363.0
	2	Sn4	335.8		1	Ba	378.1
	2	Sn5	351.4		1	Sn1	385.9
	2	Ba	363.5		1	Ba	386.6
				Sn7:	4	Co	260.4
					4	Sn5	326.9
					4	Sn6	339.0
					4	Sn1	380.8

The $Sn2@Sn_6$ octahedra are located in the larger voids left by the $[Co_4Sn_{15}]$ network. Taking into account both the Co–Sn and Sn–Sn bonding, one can describe the $BaCo_2Sn_8$ structure also by a three-dimensional $[Co_2Sn_8]$ network in which the barium atoms fill larger cavities. The barium atoms have only tin neighbors. The Ba–Sn distances for the 13 neighbors range from 352 to 399 pm, slightly longer than the sum of the covalent radii [23] of 338 pm. Similar high coordination numbers occur for the barium atoms in $BaSn_5$ (2×355 and 12×373 pm) [31] which crystallizes with an ordered superstructure of the AlB_2 type.

The coordination polyhedron of the barium atom is derived from a cuboctahedron in which one of the triangles is substituted by a rectangle, thus increasing the coordination number from 12 to 13. Similar coordination is observed in the structure of UAl_4 [32]. Always two of such $Ba@Sn_{13}$ polyhedra are condensed *via* a common rectangular face forming a double unit. The latter are further condensed *via* trans-standing rectangular faces, leading to a chain-like motif (Fig. 5). Adjacent chains are condensed *via* common edges to

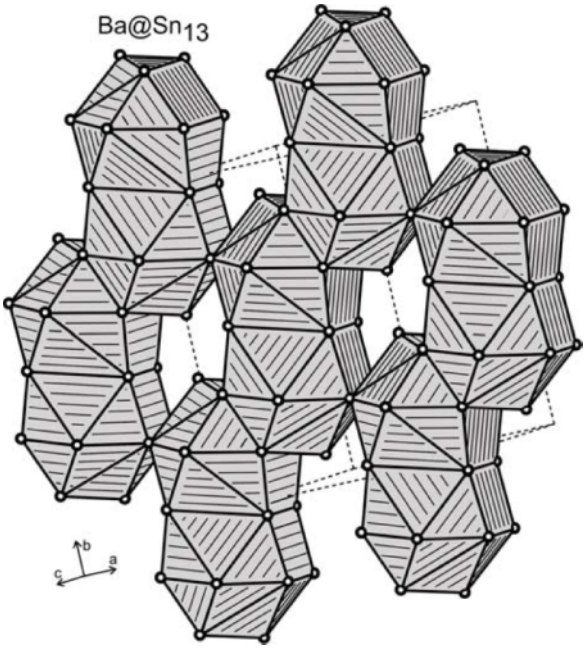

Fig. 5. Cutout of the $BaCo_2Sn_8$ structure. One layer of condensed $Ba@Sn_{13}$ polyhedra is emphasized. For details see text.

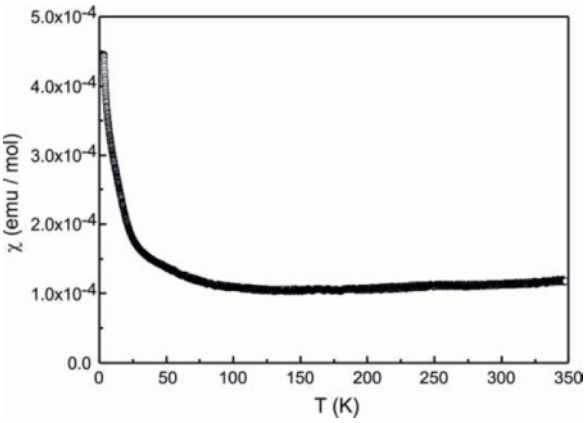

Fig. 6. Temperature dependence of the magnetic susceptibility of $BaCo_2Sn_8$ measured at an applied field of 10 kOe.

a layer-like substructure. These layers are connected with the neighboring layers (not shown in Fig. 5 for reasons of clarity) *via* common corners.

Magnetic properties of $BaCo_2Sn_8$

The temperature dependence of the susceptibility data (χ) of $BaCo_2Sn_8$, measured at an applied field of 10 kOe, is displayed in Fig. 6. The course of the susceptibility data can be considered temperature independent above 100 K. The increase in susceptibility at low temperatures is most likely due to small amounts of paramagnetic impurities. A fit of the data in the temperature range of 3 – 350 K with a modified Curie-Weiss law results in $\mu_{\text{eff}} = 0.10(1)\ \mu_B$ per formula unit, a Weiss constant $\theta_P = -3.2(5)$ K, and a temperature-independent contribution $\chi_0 = 9.8 \times 10^{-5}$ emu mol^{-1}. $BaCo_2Sn_8$ can therefore be classified as a Pauli paramagnet.

Acknowledgement

We thank Dipl.-Ing. U. Ch. Rodewald for the single-crystal data collection. This work was supported by the Deutsche Forschungsgemeinschaft.

[1] H. Rajeswari, H. Manohar, *Ind. J. Pure Appl. Phys.* **1970**, *8*, 363.
[2] O. Nial, *Z. Anorg. Allg. Chem.* **1938**, *238*, 287.
[3] A. Lang, W. Jeitschko, *Z. Metallkd.* **1996**, *87*, 759.
[4] R. V. Skolozdra in *Handbook on the Physics and Chemistry of Rare Earths* (Eds.: K. A. Gschneidner Jr., L. Eyring), Elsevier Science, Amsterdam, **1997**, Chapter 164, pp. 399 – 517.
[5] M. G. Kanatzidis, R. Pöttgen, W. Jeitschko, *Angew. Chem. Int. Ed.* **2005**, *44*, 6996.
[6] R. Pöttgen, *Z. Naturforsch.* **2006**, *61b*, 677.
[7] P. Villars, K. Cenzual, *Pearson's Crystal Data – Crystal Structure Database for Inorganic Compounds*, Release 2011/12, ASM International, Materials Park, Ohio, USA, **2012**.
[8] R. Pöttgen, Zh. Wu, R.-D. Hoffmann, G. Kotzyba, H. Trill, J. Senker, D. Johrendt, B. D. Mosel, H. Eckert, *Heteroatom Chem.* **2002**, *13*, 506.
[9] R. Pöttgen, T. Dinges, H. Eckert, P. Sreeraj, H.-D. Wiemhöfer, *Z. Phys. Chem.* **2010**, *224*, 1475.
[10] V. Hlukhyy, H. He, L.-A. Jantke, T. F. Fässler, *Chem. Eur. J.* **2012**, *18*, 12000.
[11] M. Schreyer, G. Kraus, T. F. Fässler, *Z. Anorg. Allg. Chem.* **2004**, *630*, 2520.
[12] G. Krauss, Q. F. Gu, *J. Solid State Chem.* **2008**, *181*, 2058.
[13] A. S. Cooper, *Mater. Res. Bull.* **1980**, *15*, 799.
[14] G. P. Espinosa, A. S. Cooper, H. Barz, *Mater. Res. Bull.* **1982**, *17*, 963.
[15] M. Schreyer, T. F. Fässler, *Solid State Sci.* **2006**, *8*, 793.
[16] T. Mishra, C. Schwickert, T. Langer, R. Pöttgen, *Z. Naturforsch.* **2011**, *66b*, 664.
[17] R. Pöttgen, Th. Gulden, A. Simon, *GIT Labor-Fachzeitschrift* **1999**, *43*, 133.
[18] K. Yvon, W. Jeitschko, E. Parthé, *J. Appl. Crystallogr.* **1977**, *10*, 73.
[19] G. M. Sheldrick, SHELXS-97, Program for the Solution of Crystal Structures, University of Göttingen, Göttingen (Germany) **1997**.
[20] G. M. Sheldrick, *Acta Crystallogr.* **1990**, *A46*, 467.
[21] G. M. Sheldrick, SHELXL-97, Program for the Refinement of Crystal Structures, University of Göttingen, Göttingen (Germany) **1997**.
[22] G. M. Sheldrick, *Acta Crystallogr.* **2008**, *A64*, 112.
[23] J. Emsley, *The Elements*, Oxford University Press, Oxford **1999**.
[24] R. Pöttgen, *Z. Naturforsch.* **1995**, *50b*, 175.
[25] M. Pani, P. Manfrinetti, A. Palenzona, S. K. Dhar, S. Singh, *J. Alloys Compd.* **2000**, *299*, 39.
[26] X.-W. Lei, G.-H, Zhong, M.-J. Li, J.-G. Mao, *J. Solid State Chem.* **2008**, *181*, 2448.
[27] J. Donohue, *The Structures of the Elements,* Wiley, New York **1974**.
[28] D. Niepmann, R. Pöttgen, K. M. Poduska, F. J. DiSalvo, H. Trill, B. D. Mosel, *Z. Naturforsch.* **2001**, *56b*, 1.
[29] R.-D. Hoffmann, D. Kußmann, U. Ch. Rodewald, R. Pöttgen, C. Rosenhahn, B. D. Mosel, *Z. Naturforsch.* **1999**, *54b*, 709.
[30] F. Zürcher, R. Nesper, S. Hoffmann, T. F. Fässler, *Z. Anorg. Allg. Chem.* **2001**, *627*, 2211.
[31] T. F. Fässler, S. Hoffmann, C. Kronseder, *Z. Anorg. Allg. Chem.* **2001**, *627*, 2486.
[32] B. S. Borie, Jr., *Trans. Am. Inst. Min. Metall. Pet. Eng.* **1951**, *191*, 800.